Magnetostratigraphic data on Neogene growth folding in the foreland basin of the southern Tianshan Mountains

Jimin Sun[1,*], Yang Li[2], Zhenqing Zhang[1], and Bihong Fu[1]
[1]Key Laboratory of Cenozoic Geology and Environment, Institute of Geology and Geophysics, Chinese Academy of Sciences, P.O. Box 9825, Beijing 100029, China
[2]Department of Oilfield Exploration and Development, Sinopec, Beijing 100029, China

ABSTRACT

The Tianshan Range is one of the longest and highest mountain belts in Central Asia, stretching east-west for ~2500 km. Uplift of this late Paleozoic orogenic belt resulted from intracontinental deformation caused by the collision of the Indian and Eurasian plates during the Cenozoic era. To constrain the timing of Cenozoic tectonic deformation of the Tianshan Range, we analyzed the magnetostratigraphy of 3780-m-thick Neogene deposits from the Kuqa foreland basin of southern Tianshan. The geometry measurements and magnetic fabric data show that syntectonic growth strata began to accumulate at ~6.5 Ma ago, indicating that crustal shortening initiated in the latest Miocene. The increase in sedimentation rate and an abrupt change of the magnetic fabric parameters also occurred at 6.5 Ma, accompanied by onset of syntectonic growth strata. The latest Miocene crustal shortening is a significant tectonic event in the foreland basin of the southern Tianshan Range in response to the India-Eurasia collision.

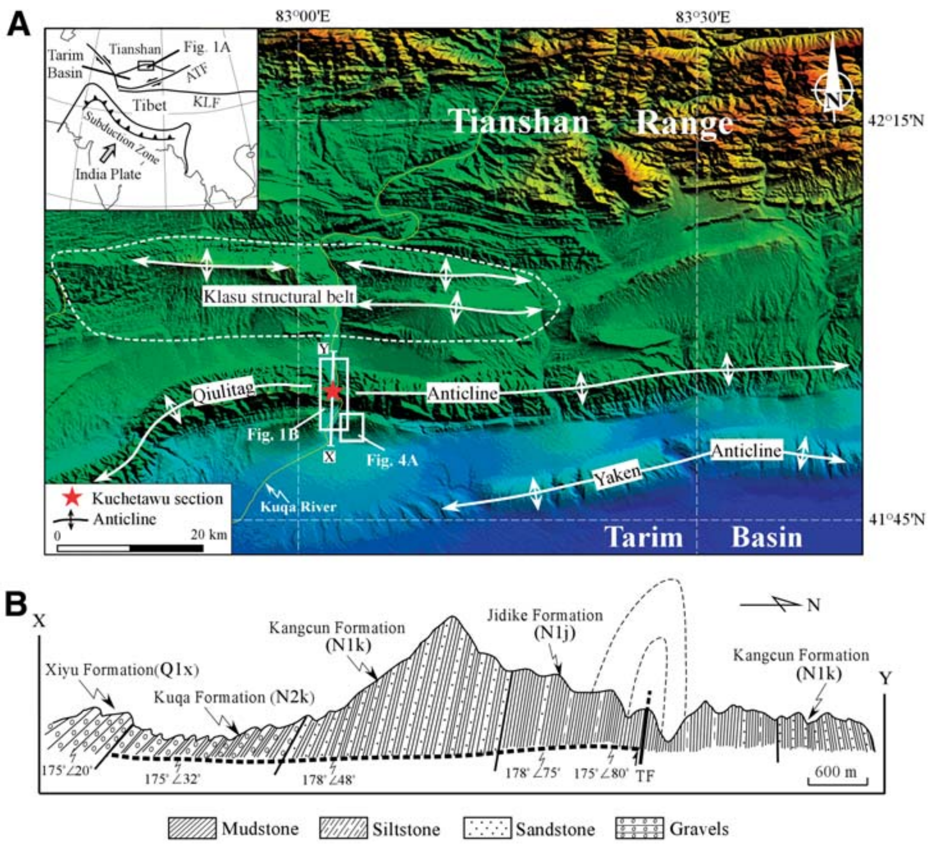

Figure 1. (A) Map showing site location of Kuchetawu section and anticlines in Kuqa foreland basin of southern Tianshan Range; inset figure shows regional tectonic map of Indian-Eurasian convergence zone. (B) Cenozoic strata of Kuchetawu section along cross-section X–Y (location in A); bold dashed line indicates our sampling route. ATF—Altyn Tagh fault; KLF—Kunlun fault; N1j—middle Miocene Jidike Formation; N1k—late Miocene Kangcun Formation; N2k—Pliocene Kuqa Formation; Q1x—early Pleistocene Xiyu Formation; TF—thrust fault.

INTRODUCTION

The Cenozoic tectonic uplift of the Tianshan Range was a response to the intracontinental deformation within the India-Eurasia convergent system (Fig. 1A). Active faulting and folding affects the northern and southern foreland basins of the Tianshan Range, indicating Cenozoic crustal shortening (Molnar and Tapponnier, 1975). The exact timing of deformation of the Tianshan Range has been an important issue in recent years (e.g., Tapponnier and Molnar, 1979; Yin et al., 1998; Deng et al., 2000; Burchfiel et al., 1999; Chen et al., 2002; Fu et al., 2003; Sun et al., 2004, 2007; Sun and Zhang, 2009; Charreau et al., 2005, 2006; Huang et al., 2006; Sobel et al., 2006; Hubert-Ferrari et al., 2007), and different opinions about the timing of major uplift exist, ranging from the late Oligocene to the early Pleistocene. Such differences are either due to the different methods used to infer age of shortening or to the nonsynchronous deformation associated with tectonic propagation from the mountains to the foreland basins.

In foreland basins, growth strata are closely linked to folding and faulting, and, thus, syntectonic sediments can provide precise information on tectonic and depositional interaction (Suppe et al., 1992; Burbank et al., 1996). When examinations of growth strata are combined with high-resolution age determinations defined by magnetostratigraphy of the syntectonic deposits, the age of tectonic deformation in foreland basins can be elucidated.

The aims of this paper are to: (1) construct a high-resolution magnetostratigraphy of Upper Cenozoic deposits in the Kuqa foreland basin, (2) define the geometry of the deformed strata to identify syntectonic deposits, (3) provide precise chronology of growth strata in the foreland basin; and (4) explore the coupling mechanisms between syntectonic sedimentation and related faulting and folding.

GEOLOGIC SETTING AND LITHOLOGY

The Kuqa foreland basin is defined by the Tianshan Mountains to the north and Tarim Basin to the south (Fig. 1A). Series of elongated anticlines parallel to the Tianshan orogenic belt indicate ongoing north-south contraction and crustal shortening. Here, we focus on the Kuchetawu section (41°55.097′N, 83°03.280′E), which is part in the Qiulitag anticline, exposed (transect

*E-mail: jmsun@mail.igcas.ac.cn.

Geology, November 2009; v. 37; no. 11; p. 1051–1054; doi: 10.1130/G30278A.1; 4 figures.

X–Y, Fig. 1A) by the southward-flowing Kuqa River (Fig. 1A). Field investigations indicate that in this section the Qiulitag anticline is an overturned fold, consisting of steep strata in the core and gentle dip strata in the limbs (Fig. 1B). This anticline exposes the early Miocene Jidike Formation (N1j), the late Miocene Kangcun Formation (N1k), the Pliocene Kuqa Formation (N2k), and the early Pleistocene Xiyu Formation (Q1x). Generally, there is a trend toward coarser particle size and more gravels from core to limbs (Fig. 1B).

RESULTS

Paleomagnetic sampling focused on the southern limb of the Kuchetawu anticline (Fig. 1B). In total, 676 oriented samples were subjected to stepwise thermal demagnetization; in 650 specimens, the characteristic remanent magnetization (ChRM) was successfully isolated after removal of one or two secondary components of magnetization. For most samples, two magnetic components were isolated. A low-temperature magnetic component was removed by thermal demagnetization at ~200–250 °C, and another component above 250 °C carried the ChRM direction. The ChRM vector directions were used to define magnetostratigraphic polarity.

The age of the sequence is further constrained by the occurrence of vertebrate fossil *Hipparion chiai* at a depth of 3100 m (Fig. 2). This kind of fossil corresponds to the Vallesian age of European Neogene mammal zones (MN) 9/10 (Deng, 2006), which have an age range of 11–9 Ma, centered at ca. 10 Ma. Finally, the extremely thick (>1000 m) conglomerate sequence of the Xiyu Formation is a marker stratum in northwestern China. Its basal age has been proposed to be near the Pliocene-Pleistocene boundary (e.g., Huang et al., 1947).

Combined with these age controls, the measured magnetic polarity sequence was correlated to the geomagnetic polarity time scale (GPTS) of Cande and Kent (1995) (Fig. 2). The magnetozones of sampled sediments correlate with polarity chrons from the topmost of C5ABn to C2An.1n, covering an age range of 13.3–2.6 Ma.

We also measured the anisotropy of magnetic susceptibility (AMS) of 648 samples using the KLY-3s Kappabridge with a CS-3 high-temperature furnace in an argon atmosphere. Magnetic fabrics of deformed rocks can reflect the strain state of rocks (e.g., Graham, 1954; Tarling and Hrouda, 1993; Parés and van der Pluijm, 2002). In this study, the overall magnetic fabric parameters, except the mean magnetic susceptibility (k_m), show distinct patterns before and after 6.5 Ma (Fig. 3).

DISCUSSION

Mountains and adjoining foreland basins are coupled systems. Foreland basins not only accommodate sediment eroded off adjacent mountains, accumulating as thick sedimentary successions, but they also undergo progressive deformation in response to crustal shortening. In this sense, the sequences at the edges of foreland basins document the tectonic deformation history. Studies of the geometry and chronology of deformed strata can provide information about the timing of deformation as well as the interplay between sedimentation and crustal shortening.

Growth strata are developed in the southern limb of the Kuchetawu anticline. Syntectonic sediments accumulated from the upper part of the Kangcun Formation to the Lower Pleistocene Xiyu Formation (Fig. 4A). The growth strata are characterized by (1) dips of strata that become shallower gradually southward, decreasing from ~60° to 40° in the upper part of the Kangcun Formation to ~40° to 28° in the Kuqa Formation and then decreasing to ~22°–20° for the Xiyu Formation (Fig. 4A); (2) thinner strata toward the crest, indicating that they accumulated during deformation; and (3) a series of progressive and syntectonic onlap angular unconformities (typical features of growth strata) that show the tectonic deformation propagated southward to the Kuqa Foreland basin. Based on the magnetostratigraphic data, the age of inception of growth strata is around 6.5 Ma (Figs. 2 and 4A). Therefore, the syntectonic deposits began to accumulate ca. 6.5 Ma, and those processes continued to the early Pleistocene. This new result

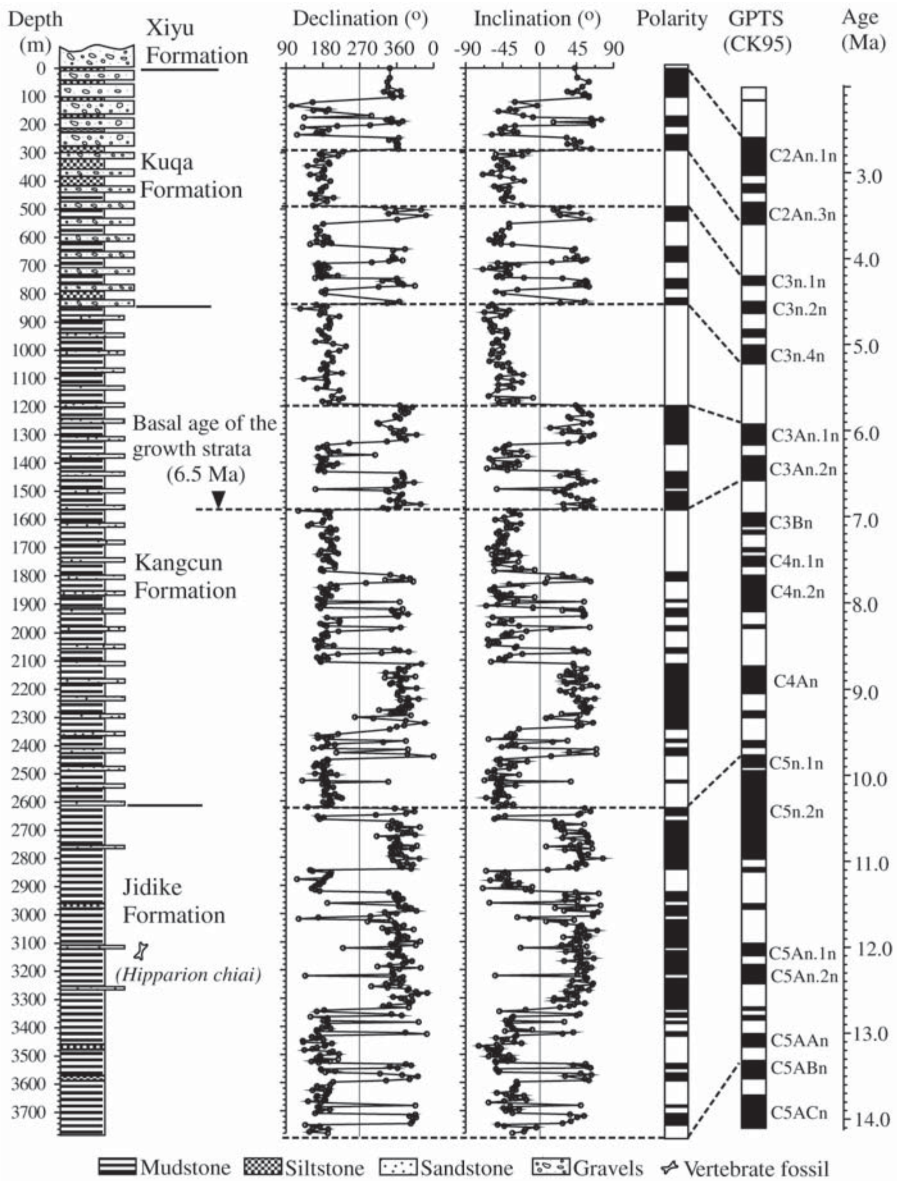

Figure 2. Magnetostratigraphy of Kuchetawu section. Magnetic polarity is compared with geomagnetic polarity time scale (GPTS) of Cande and Kent (1995). Vertebrate fossil *Hipparion chiai* at a depth of 3100 m suggests an age of ca. 10 Ma.

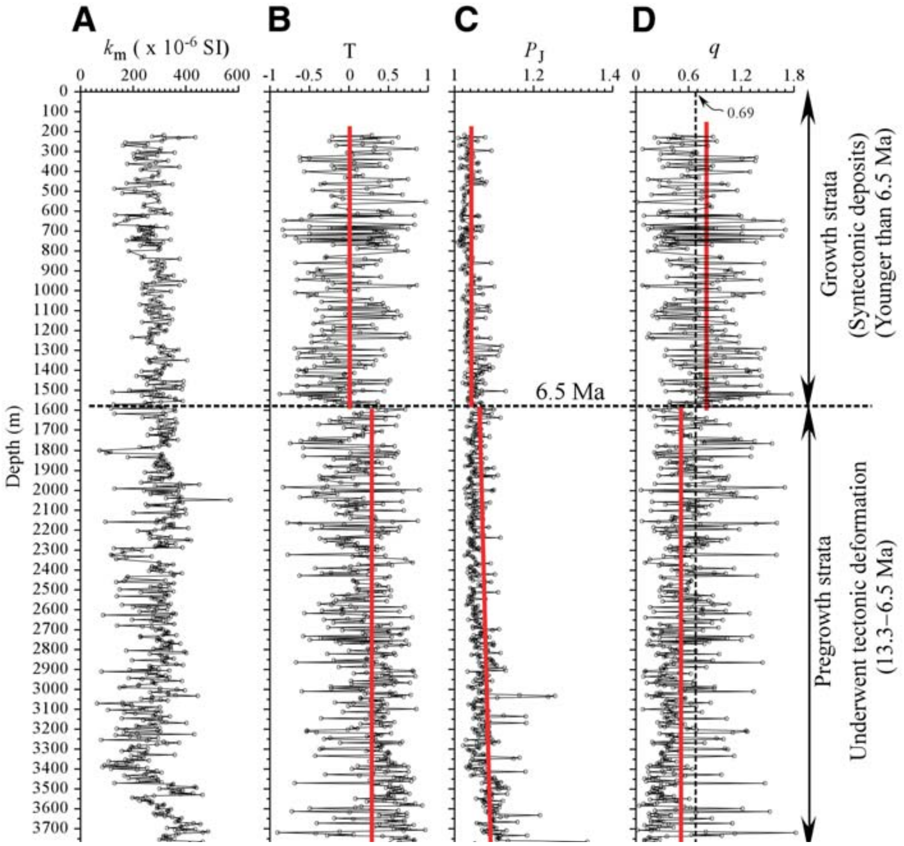

Figure 3. Magnetic fabric data from Kuchetawu section. Mean magnetic susceptibility (k_m) and magnetic anisotropic parameters of T, P_J, and q are shown as a function of depth, noting abrupt changes of three later parameters since 6.5 Ma.

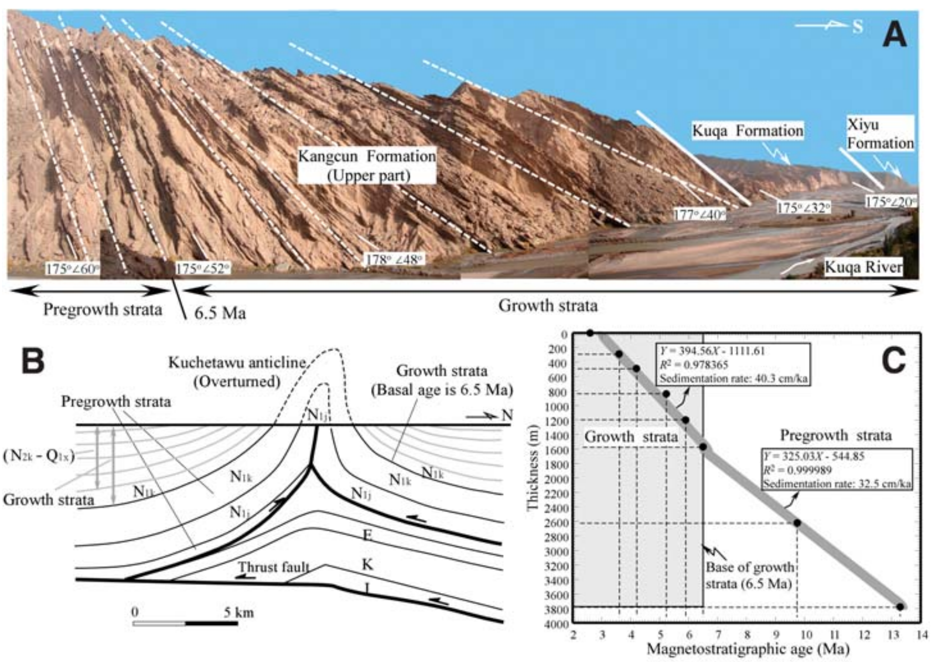

Figure 4. (A) Growth strata (from upper part of Kangcun Formation to Xiyu Formation) from ca. 6.5 Ma to early Pleistocene exposed along southern limb of Kuchetawu anticline. (B) Deep and shallow structures of Kuchetawu anticline based on interpretation of seismic-reflection profiles; accumulation of syntectonic growth strata is mainly associated with upper thrust faults. (C) Thickness as a function of magnetostratigraphic age from Kuchetawu anticline; a distinct increase in accumulation rate is indicated at 6.5 Ma.

from the southern Tianshan is consistent with the dated syntectonic growth strata in the middle part of northern Tianshan, which indicate an age of 6 Ma (Sun and Zhang, 2009), but it is earlier than the reported 5.5 Ma growth strata of the Yaken anticline in the southern Tianshan (Hubert-Ferrari et al., 2007).

The seismic-reflection profile of this anticline (Fig. 4B) shows that the anticline is a fault-related fold, and it has two distinct structural levels. The deeper structure is a typical fault-bend fold, where the deep detachment fault steps southward along an Upper Jurassic coal bed at a depth of ~9 km; the upper anticline is controlled by both the back thrust in the forelimb and the south thrust fault in the backlimb (Fig. 4B). These two faults, rooted in the gypsum layer of the Miocene Jidike Formation, merge near the surface and have near-vertical dips (Fig. 4B). The growth strata accumulated on the hanging wall of the faults penecontemporaneously with folding of the pregrowth strata older than 6.5 Ma.

Magnetostratigraphic age controls allow us to calculate sedimentation rates (Fig. 4C). The sedimentation rate of pregrowth strata is 32.5 cm/ka and increases to 40.3 cm/ka at 6.5 Ma, when growth strata accumulated. The coincidence of the syntectonic growth strata and the increased sedimentation rate demonstrates that the southern Tianshan experienced crustal shortening in response to intracontinental deformation within the India and Eurasia convergent system initiated 6.5 Ma ago and continuing into the early Pleistocene.

The tectonic deformation can be also demonstrated by the AMS data (Fig. 3). The AMS of sediments depends on the preferred orientation of strongly magnetic minerals, which is affected by both depositional processes and tectonic deformation. AMS has been widely used to infer the geodynamic settings of various environments (Tauxe et al., 1998). The vertical variations of the AMS parameters of T (shape parameter), P_J (corrected anisotropy degree), and q (another shape parameter) do not correlate with changes in mean magnetic susceptibility km (Fig. 3A), suggesting that they are independent of the ferromagnetic concentrations in the succession. The changes in AMS parameters at ~6.5 Ma are not controlled by sedimentary fabrics. Moreover, although the magnetic properties of the sediments may be also driven by climate change, the mean susceptibility variations are generally rather stable (Fig. 3A). This is not consistent with the climatic cooling trend of the late Cenozoic. Therefore, it does not support climatic control of AMS.

The AMS T parameter is lower in sediments younger than 6.5 Ma (Fig. 3B): the mean value decreases from 0.217 to 0.001 after ca. 6.5 Ma. Values of $T > 0$ correspond to oblate (disk) shapes; those with T < 0 indicate prolate (rod) shapes. The observed changes in T show dominantly oblate fabric from the base to a depth of 1570 m (from 13.3 to 6.5 Ma in age) (Fig. 3B). Similar trends are also observed for the corrected anisotropy degree (P_J) (Fig. 3C). If T and P_J are dominated by postsedimentary fabric, e.g., due to compaction, then both should show increasing trends from the top to a depth of 1570 m (from 2.6 to 6.5 Ma in age). However, this is not the case. The observed abrupt changes of AMS parameters at 6.5 Ma are not a predominant sedimentologic factor. Another shape parameter q displays very different trends compared with the changes of T and P_J (Fig. 3D). This parameter generally shows higher values (mean value is 0.73) above 1570 m and lower values (mean value is 0.53) in sediments older than 6.5 Ma. When $q < 0.69$, the fabric is oblate, and when $q > 0.69$ the fabric is prolate (Tarling and Hrouda, 1993). The ellipsoid shapes are dominantly oblate earlier than 6.5 Ma ago, and then they change to dominant prolate shapes after 6.5 Ma (Fig. 3D).

We propose the following mechanism to account for the abrupt changes in AMS parameters. Sediments older than 6.5 Ma are presyntectonic strata, and they experienced contraction due to crustal shortening. Obviously, the magnetic anisotropy of these strata was affected by stress, and the tectonic fabrics were superimposed on the primary predeformational magnetic fabric as a result of later deformation. The degree of magnetic anisotropy increased with increasing intensity of strain. This can explain the general increasing trend of T and P_J for the sediments from 6.5 to 13.3 Ma, as well as the dominant oblate shapes earlier than 6.5 Ma (Fig. 3).

The past 6.5 Ma of growth strata were deposited during crustal shortening. As syntectonic deposits, their magnetic fabric was mainly controlled by sedimentation, and thus they exhibit lower degree of anisotropy and less oblate shapes (Fig. 3).

Although structural deformation in the foreland basin of the Tianshan Mountains was initiated in the early Miocene (e.g., Allen et al., 1991; Avouac et al., 1993; Hendrix et al., 1994; Sobel and Dumitru 1997; Yin et al., 1998; Sobel et al., 2006), the timing of tectonic deformation in different areas of the foreland basin should not be synchronous due to fault propagation. Our results demonstrate that latest Miocene tectonic deformation must have been an important episode of crustal shortening in the Tianshan Range, lasting from ca. 6.5 Ma to the early Pleistocene, as a consequence of intracontinental deformation within the India-Eurasia convergent system.

ACKNOWLEDGMENTS

This study was supported by Projects KZCX2-YW-130 and KZCX2-YW-Q09-06-04 from the Chinese Academy of Sciences, and the National Natural Science Foundation of China (grants 40830104 and 40772115). We thank R.X. Zhu and Q.S. Liu for helpful discussions, and the two reviewers for constructive reviews and language improvements.

REFERENCES CITED

Allen, M.B., Windley, B.F., Zhang, C., Zhao, Z., and Wang, G., 1991, Basin evolution within and adjacent to the Tien Shan range, NW China: Journal of the Geological Society of London, v. 148, p. 369–378, doi: 10.1144/gsjgs.148.2.0369.

Avouac, J.P., Tapponnier, P., Bai, M., Hou, Y., and Wang, G., 1993, Active thrusting and folding along the northeastern Tienshan, and rotation of Tarim relative to Dzungaria and Kazakhstan: Journal of Geophysical Research, v. 98, p. 6755–6804, doi: 10.1029/92JB01963.

Burbank, D., Meigs, A., and Brozovic, N., 1996, Interaction of growing folds and coeval depositional systems: Basin Research, v. 8, p. 199–223, doi: 10.1046/j.1365-2117.1996.00181.x.

Burchfiel, B.C., Brown, E.T., Deng, Q.D., Feng, X.Y., Li, J., Molnar, P., Shi, J.B., Wu, Z.M., and You, H.C., 1999, Crustal shortening on the margins of the Tien Shan, Xinjiang, China: International Geology Review, v. 41, p. 665–700, doi: 10.1080/00206819909465164.

Cande, S.C., and Kent, D.V., 1995, Revised calibration of the geomagnetic polarity timescale for the Late Cretaceous and Cenozoic: Journal of Geophysical Research, v. 100, p. 6093–6095, doi: 10.1029/94JB03098.

Charreau, J., Chen, Y., Gilder, S., Dominguez, S., Avouac, J.P., Sen, S., Sun, D.J., Li, Y.A., and Wang, W.M., 2005, Magnetostratigraphy and rock magnetism of the Neogene Kuitun He section (northwest China): Implications for late Cenozoic uplift of the Tianshan mountains: Earth and Planetary Science Letters, v. 230, p. 177–192, doi: 10.1016/j.epsl.2004.11.002.

Charreau, J., Gilder, S., Chen, Y., Dominguez, S., Avouac, J.P., Sen, S., Jolivet, M., Li, Y., and Wang, W., 2006, Magnetostratigraphy of the Yaha section, Tarim Basin (China): 11 Ma acceleration in erosion and uplift of the Tian Shan mountains: Geology, v. 34, p. 181–184, doi: 10.1130/G22106.1.

Chen, J., Burbank, D.W., Scharer, K.M., Sobel, E., Yin, J.H., Rubin, C., and Zhao, R.B., 2002, Magnetochronology of the Upper Cenozoic strata in the southwestern Chinese Tian Shan: Rates of Pleistocene folding and thrusting: Earth and Planetary Science Letters, v. 195, p. 113–130, doi: 10.1016/S0012-821X(01)00579-9.

Deng, Q.D., Feng, X.Y., Zhang, P.Z., Xu, X.W., Yang, X.P., Peng, S.Z., and Li, J., 2000, Active Tectonics of the Chinese Tianshan Mountains: Beijing, Seismology Press, 399 p.

Deng, T., 2006, Chinese Neogene mammal biochronology: Vertebrate PalAsiatic, v. 44, p. 143–163.

Fu, B.H., Lin, A.M., Kano, K., Maruyama, T., and Guo, J.M., 2003, Quaternary folding of the eastern Tianshan, Northwest China: Tectonophysics, v. 369, p. 79–101, doi: 10.1016/S0040-1951(03)00137-9.

Graham, J.W., 1954, Magnetic susceptibility anisotropy, an unexploited petrofabric element: Geological Society of America Bulletin, v. 65, p. 1257–1258.

Hendrix, M.S., Dumitru, T.A., and Graham, S.A., 1994, Late Oligocene–early Miocene unroofing in the Chinese Tian Shan: An early effect of the India-Asia collision: Geology, v. 22, p. 487–490, doi: 10.1130/0091-7613(1994)022<0487:LOEMUI>2.3.CO;2.

Huang, B.C., Piper, J.D.A., Peng, S.T., Liu, T., Li, Z., Wang, Q.C., and Zhu, R.X., 2006, Magnetostratigraphic study of the Kuche Depression, Tarim Basin, and Cenozoic uplift of the Tian Shan Range, Western China: Earth and Planetary Science Letters, v. 251, p. 346–364, doi: 10.1016/j.epsl.2006.09.020.

Huang, T.K., Young, C.C., Cheng, Y.C., Chow, T.C., Bien, M.N., and Weng, W.P., 1947, Report on Geological Investigation of Some Oil-Fields in Sinkiang (Geology Memoirs, Series A, No. 21): Nanking, The National Geology Survey China, 118 p.

Hubert-Ferrari, A., Suppe, J., Gonzalez-Mieres, R., and Wang, X., 2007, Mechanisms of active folding of the landscape (southern Tian Shan, China): Journal of Geophysical Research, v. 112, p. B03S09, doi: 10.1029/2006JB004362.

Molnar, P., and Tapponnier, P., 1975, Cenozoic tectonics of Asia: Effects of a continental collision: Science, v. 189, p. 419–426, doi: 10.1126/science.189.4201.419.

Parés, J.M., and van der Pluijm, B., 2002, Evaluating magnetic lineations (AMS) in deformed rocks: Tectonophysics, v. 350, p. 283–298, doi: 10.1016/S0040-1951(02)00119-1.

Sobel, E.R., and Dumitru, T.A., 1997, Thrusting and exhumation around the margins of the western Tarim Basin during the India-Asia collision: Journal of Geophysical Research, v. 102, p. 5043–5063, doi: 10.1029/96JB03267.

Sobel, E.R., Chen, J., and Heermance, R.V., 2006, Late Oligocene–early Miocene initiation of shortening in the southwestern Chinese Tian Shan: Implications for Neogene shortening rate variations: Earth and Planetary Science Letters, v. 247, p. 70–81, doi: 10.1016/j.epsl.2006.03.048.

Sun, J.M., and Zhang, Z.Q., 2009, Syntectonic growth strata and implications for late Cenozoic tectonic uplift in the northern Tian Shan, China: Tectonophysics, v. 463, p. 60–68, doi: 10.1016/j.tecto.2008.09.008.

Sun, J.M., Zhu, R.X., and Bowler, J., 2004, Timing of the Tianshan Mountains uplift constrained by magnetostratigraphic analysis of molasse deposits: Earth and Planetary Science Letters, v. 219, p. 239–253, doi: 10.1016/S0012-821X(04)00008-1.

Sun, J.M., Xu, Q.H., and Huang, B.C., 2007, Late Cenozoic magnetochronology and paleoenvironmental changes in the northern foreland basin of the Tian Shan Mountains: Journal of Geophysical Research, v. 112, doi: 10.1029/2006JB004653.

Suppe, J., Chou, G.T., and Hook, S.C., 1992, Rates of folding and faulting determined from growth strata, *in* McClay, K.R., ed., Thrust Tectonics: Suffolk, Chapman & Hall, p. 105–121.

Tapponnier, P., and Molnar, P., 1979, Active faulting and Cenozoic tectonics of the Tien Shan, Mongolia, and Baykal regions: Journal of Geophysical Research, v. 84, p. 3425–3459, doi: 10.1029/JB084iB07p03425.

Tarling, D.H., and Hrouda, F., 1993, The Magnetic Anisotropy of Rocks: London, Chapman and Hall, 217 p.

Tauxe, L., Gee, J.S., and Staudigel, H., 1998, Flow directions in dikes from anisotropy of magnetic susceptibility data: The bootstrap way: Journal of Geophysical Research, v. 103, p. 17,775–17,790, doi: 10.1029/98JB01077.

Yin, A., Nie, S., Craig, P., Harrison, T.M., Ryerson, F.J., Qian, X., and Yang, G., 1998, Late Cenozoic tectonic evolution of the southern Chinese Tian Shan: Tectonics, v. 17, p. 1–27, doi: 10.1029/97TC03140.

Manuscript received 30 March 2009
Revised manuscript received 19 June 2009
Manuscript accepted 30 June 2009

Printed in USA